Chaotic Dynamics of Ballistic Electrons in Lateral Superlattices and Magnetic Fields

T. Geisel,[1] J. Wagenhuber,[1] P. Niebauer,[2] and G. Obermair[2]

[1]*Institut für Theoretische Physik, Universität Regensburg, D-8400 Regensburg, Federal Republic of Germany and Institut für Theoretische Physik and Sonderforschungsbereich Nichtlineare Dynamik, Universität Frankfurt, D-6000 Frankfurt, Federal Republic of Germany*[a]

[2]*Institut für Festkörperphysik, Universität Regensburg, D-8400 Regensburg, Federal Republic of Germany*

(Received 18 December 1989)

We study the classical dynamics of a ballistic charged particle in a two-dimensional (2D) periodic potential and an applied magnetic field. We find chaotic behavior, in particular in the form of normal diffusion and anomalous diffusion associated with $1/f$ noise. The mechanisms for the onset of 1D diffusion and 2D diffusion are explained in terms of homoclinic intersections and Kolmogorov-Arnol'd-Moser theory. The model may be used as a classical approximation for ballistic-electron dynamics in lateral superlattices on semiconductor heterojunctions.

PACS numbers: 73.40.Kp, 05.40.+j, 05.45.+b

The dynamics of charged particles in two-dimensional (2D) periodic potentials and perpendicular magnetic fields gives rise to a variety of interesting phenomena. Based on the Peierls-Onsager hypothesis Hofstadter demonstrated that the quantum states may exhibit a self-similar band structure depending on the incommensurability of two characteristic length scales.[1] The corresponding quasiperiodic Schrödinger operator may have a spectrum with a singular continuous component[2] and the wave functions may be critical or exotic, i.e., neither extended nor localized.[3] To circumvent unaccessibly strong magnetic fields Hofstadter suggested study of artificial 2D superlattices with much larger lattice spacing than in natural crystals.[1] On the other hand, as the lattice spacing increases with respect to the Fermi wavelength, the wave-packet dynamics approaches the classical limit. With the present possibilities to realize high-mobility heterojunctions with lateral periodic microstructures, the time has come to also ask for the classical counterpart of the problem, e.g., as an approximation for the dynamics of a ballistic electron.

In the present Letter we show that the classical counterpart of the model studied by Hofstadter and others exhibits chaotic behavior caused by a nonintegrable coupling due to the magnetic field and we point out the relevance of Kolmogorov-Arnol'd-Moser (KAM) theory[4] for the observed phenomena. In particular we find various types of chaotic diffusion, which we characterize by a power spectral analysis. As the magnetic field is increased from zero, a one-dimensional (1D) anomalous diffusion process sets in. It is accompanied by $1/f$ noise corresponding to a nonlinear growth of the mean-square displacement. For stronger fields there are transitions to normal diffusion, 2D diffusion, and 2D anomalous diffusion. Based on Poincaré surfaces of section we explain the mechanism for the onset of 1D diffusion by the generation of stochastic layers due to homoclinic intersections near the unperturbed separatrices. The transition to 2D diffusion is caused by the breakup of invariant KAM tori.

One possible application of the model is the motion of ballistic electrons in lateral superlattices on semiconductor heterojunctions.[5-8] At present these systems are studied intensely not only for academic reasons, but also for their potential use in future devices. The superlattice serves to break the lateral free-electron behavior and to produce minigaps.[5] Lateral superlattices with 1D modulations[6,7] and 2D modulations[8] have been realized with lattice parameters down to about 200 nm. The lattice parameter a is larger than the Fermi wavelength (e.g., $a/\lambda_F \approx 8$ in Ref. 6) and it is rather a problem to reduce this ratio than to increase it. The dynamics of wave packets can therefore be treated on the basis of classical approximations.[9] For a typical 2D modulating potential we have previously studied the classical chaotic dynamics in the absence of a magnetic field.[10,11] We found a new mechanism for $1/f$ noise and presented a statistical theory for its explanation. Avoiding the chaotic dynamics would require a special modulating potential consisting of two perpendicular plane waves. This situation may be realized, e.g., using the persistent photoconductivity effect.[6] Considering such an integrable potential we show here, however, that addition of a magnetic field will again cause chaotic behavior. One of our conclusions regards the elastic mean free path l_e (~ 10 μm in AlGaAs/GaAs heterojunctions[6]). The occurrence of chaotic diffusion in a regular superlattice may reduce the lengths of free paths. Other possible applications of this classical treatment are related to particle channeling, fast-ion conductors, and electrostatic plasma waves.

We consider a classical particle with charge e, mass m, and energy E moving in a 2D periodic potential under the influence of a homogeneous magnetic field $\mathbf{B}=B\mathbf{z}$, described by the Hamiltonian

$$H(x,y,p_x,p_y)=(1/2m)[(p_x+eBy/2)^2+(p_y-eBx/2)^2]+V(x,y), \quad (1)$$

where $V(x,y)=V_0[2+\cos(2\pi x/a)+\cos(2\pi y/a)]$ is an

isotropic (superlattice) potential represented by the lowest Fourier components. In the case of a semiconductor heterostructure, m represents the effective mass m^* and E the Fermi energy E_F. Measuring energy in units of V_0, lengths in units of the lattice constant a, and time in units of the inverse harmonic frequency $\omega_0=(4\pi^2V_0/a^2m)^{1/2}$ leads to scaled variables $\tilde{H}=H/V_0$, $\tilde{x}=2\pi x/a$, $\tilde{y}=2\pi y/a$, $\tilde{t}=\omega_0 t$. The equations of motion then read (omitting the tildes for convenience)

$$\dot{x}=v_x,\quad \dot{v}_x=\sin x+2\lambda v_y\,,$$
$$\dot{y}=v_y,\quad \dot{v}_y=\sin y-2\lambda v_x\,, \tag{2}$$

corresponding to the Hamiltonian

$$H(x,y,p_x,p_y)=(p_x+\lambda y)^2/2+(p_y-\lambda x)^2/2+V(x,y)\,, \tag{3}$$

$$V(x,y)=2+\cos x+\cos y\,. \tag{4}$$

The dimensionless quantity

$$\lambda=eBa/(16\pi^2mV_0)^{1/2}=\omega_c/2\omega_0 \tag{5}$$

proportional to the applied magnetic field B describes the nonintegrable coupling between the 2 degrees of freedom and is related to the bare cyclotron frequency ω_c. Note that there are two integrable limits in this model, that is, $\lambda\to 0$ and $\lambda\to\infty$.

The potential V of Eq. (4) has minima at the energy $E=0$, saddle points at $E=2$, and maxima at $E=4$. Thus in the regime $E\le 2$ all orbits are restricted to one unit cell for all values of λ. For $E>2$, localized and delocalized orbits may coexist. In this article we concentrate on the intermediate energy range $2<E<4$, where qualitatively the results do not depend on the value of E. Because of space limitations we present numerical results only for the special choice $E=2.92$. In this energy range we find delocalized periodic and drifting quasiperiodic orbits coexisting with localized motions in phase space. The most interesting feature, however, is the occurrence of a variety of (deterministic) diffusive motions, which we have analyzed by means of the velocity power spectrum

$$S_a(\omega)=\frac{1}{2\pi}\int_{-\infty}^{\infty}\langle v_a(t)v_a(0)\rangle e^{i\omega t}dt\quad(a\in\{x,y\})\,, \tag{6}$$

where the angular brackets denote time averaging. We have determined $S_y(\omega)$ using the Wiener-Khinchin theorem for a set of initial conditions located in the stochastic layers (e.g., of Fig. 3). With increasing λ starting with $\lambda=10^{-4}$ we obtained the following results. For small magnetic fields ($\lambda\le 10^{-3}$) the velocity fluctuations show $1/f$ noise (see Fig. 1), i.e., a low-frequency divergence of the spectral density $S_y(\omega)\sim\omega^{-\beta}$ with $\beta\lesssim 1$ (Fig. 1, spectrum a). As explained in a previous article,[10] this must be associated with anomalous diffusion, where the mean-square displacement $\sigma_y^2(t)=\langle y^2(t)\rangle$ grows faster than linearly in time, $\sigma_y^2(t)\sim t^{1+\beta}$. Above $\lambda=10^{-3}$ there is a transition region where the character of the spectrum changes and near $\lambda=10^{-2}$ the low-frequency divergence has disappeared (Fig. 1, spectrum b). We thus can conclude that there is a transition to normal diffusion characterized by a finite value of the diffusion coefficient $D=\pi S(\omega=0)$ and by a linear growth of the mean-square displacement. Inspection of the orbits in the above two cases shows that the particle diffuses along one axis only and remains confined in the perpendicular direction. At a critical field strength $\lambda_c\approx 0.014$ there is a transition from 1D diffusion to 2D diffusion, where the particle performs a random walk in the x-y plane. With increasing values of λ the 2D diffusion becomes anomalous (see Fig. 1, spectrum c) and a normal regime is reached again above $\lambda\approx 0.3$.

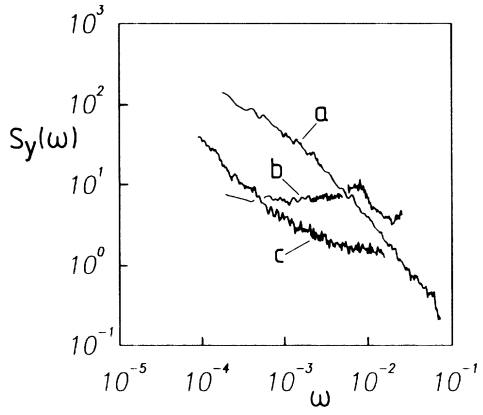

FIG. 1. Velocity power spectra $S_y(\omega)$ for various magnetic field strengths λ. For (a) $\lambda=10^{-3}$ and (c) $\lambda=0.07$, $S_y(\omega)$ diverges as $\omega^{-\beta}$ with $\beta\approx 1$ corresponding to anomalous diffusion. For (b) $\lambda=10^{-2}$, $S_y(\omega)$ remains finite for $\omega\to 0$ corresponding to normal diffusion.

We have verified the above results independently by studying the distribution of free paths. In our simulations the diffusing trajectories could be segmented into alternating episodes of motion within a potential well and motion across a number of lattice cells. We refer to the latter as free paths. Assuming them as independent events we describe their distribution by a probability density $\psi_a(t)$, where $\psi_a(t)dt$ equals the fraction of paths parallel to the a axis with duration between t and $t+dt$ ($a\in\{x,y\}$). For computational reasons we only use the integrated probability density

$$\Phi_a(t)=\int_t^{\infty}\psi_a(s)ds\,. \tag{7}$$

It can be shown[12] that the velocity power spectrum and the integrated probability density are related by

$$S_a(\omega)=\frac{\langle v_a^2\rangle}{\pi\langle\tau_a\rangle}\frac{1}{\omega}\int_0^{\infty}\Phi_a(t)\sin(\omega t)dt\,, \tag{8}$$

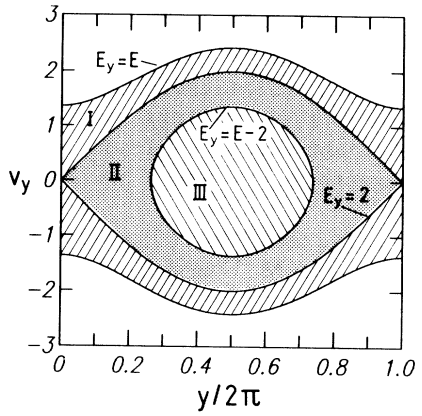

FIG. 2. Poincaré surface of section at the potential minimum for the zero-field case ($\lambda=0$). Two separatrices divide the phase space into regions of delocalized (drifting) motions (I, III) and localized motions (II).

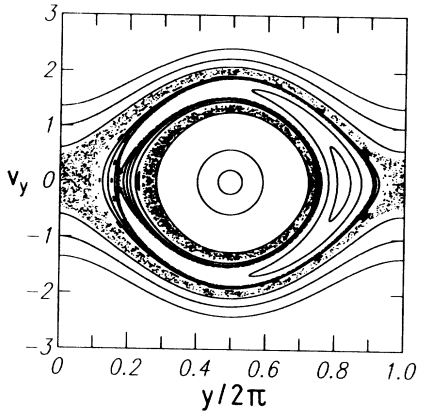

FIG. 3. Same as Fig. 2 for $\lambda=0.01$. The onset of 1D diffusion consists in the creation of stochastic layers around the two separatrices and is caused by homoclinic intersections.

where $\langle\tau_a\rangle$ is the average duration of a free path. In accordance with the above results we found that $\Phi_a(t)$ falls off exponentially $\Phi_a(t)\sim e^{-at}$ in the case of normal diffusion.[12] This leads to a Lorentzian $S_a(\omega)\sim 1/(\omega^2+a^2)$ for Eq. (8) with a finite value of $S_a(\omega=0)$. On the other hand, we observed algebraically decaying long-time tails $\Phi_a(t)\sim t^{-\nu}$ with $\nu\approx 1$ in the cases of anomalous diffusion. Equation (8) then predicts $S_a(\omega)\sim\omega^{\nu-2}$ with $\nu-2\approx -1$ in accordance with Fig. 1, spectra *a* and *c*.

We can understand the mechanisms for diffusion as well as the transitions between the regimes by analyzing the Poincaré surfaces of section (Figs. 2, 3, and 4). All sections show the y-v_y plane and $x=\pi$ (mod2π), i.e., in the potential minima. Because of the discrete translational symmetry of the potential all y coordinates (mod2π) are identified and plotted within the unit cell $[0,2\pi]$. For the total energy we can write $E=E_x+E_y$, where E_x and E_y are the instantaneous energies of each degree of freedom, e.g., $E_y=1+\cos y+v_y^2/2$. The outer boundary of the Poincaré surfaces of section is always given by the curve $E_y=E$. Consider first the zero-field case $\lambda=0$. Here the equations of motion separate into two uncoupled pendulum equations, the energies E_x and E_y are each conserved, and the orbits appear as invariant curves of constant E_y. The latter can be constructed simply from the phase portrait of the pendulum. The two pendulum separatrices for $E_y=2$ and $E_y=E-2$ (i.e., $E_x=2$) divide the plane into three regions as depicted in Fig. 2: In region I, i.e., above the y separatrix ($E_y>2$), the orbits correspond to the running solutions of the y pendulum. They are delocalized in y (drifting orbits) and thus must be localized in x (in the E range considered here). In region III, for $E_y<E-2$ we have $E_x>2$ and thus the orbits correspond to running solutions of the x pendulum and must be localized in y. Note that these two regions are interchanged under the symmetry operation $x\to y$, $y\to -x$. In the intermediate region II, we have $E_y<2$ and $E_x<2$, corresponding to swinging motion of both pendula, and the particle performs local motions in both directions. The area of localized orbits between the two separatrices decreases with increasing total energy and disappears for $E\geq 4$, when the particle energy exceeds the potential maximum. In the section there is an elliptic fixed point at $y=\pi$, $v_y=0$, corresponding to the minimum of the potential, and a hyperbolic point at $y=0$, $v_y=0$, corresponding to the saddle point of V.

As we apply a magnetic field ($\lambda>0$), in regions I and III regular drifting orbits continue to exist (Fig. 3). New elliptic and hyperbolic fixed points are created by nonlinear resonances. Stochastic layers appear at the two separatrices as expected and grow with increasing magnetic field. The sharp boundaries between regions of localized (II) and delocalized orbits (I, III) are thus destroyed and a chaotic orbit in the layer may switch from a localized to a delocalized region and vice versa. This is the origin of diffusive motion. The outer layer generates diffusion in the y direction. For symmetry reasons the inner layer plays the same role for the x direction. The stochastic layers and thus the onset of 1D diffusion are caused by a homoclinic intersection of the unstable and stable manifolds of the hyperbolic fixed point.[4]

We now turn to the mechanism for the onset of 2D diffusion. As is seen in Fig. 3 the inner and the outer stochastic layer are separated by invariant KAM tori acting as barriers. An orbit in the outer layer thus cannot reach the inner layer and a particle diffusing in the y direction cannot switch to free paths in the x direction. With increasing perturbation the KAM tori break up into cantori[13] and become partially penetrable thereby allowing 2D diffusion. Figure 4 shows the critical case $\lambda_c=0.014$ where the two stochastic layers start being connected. The rate of switching between x diffusion

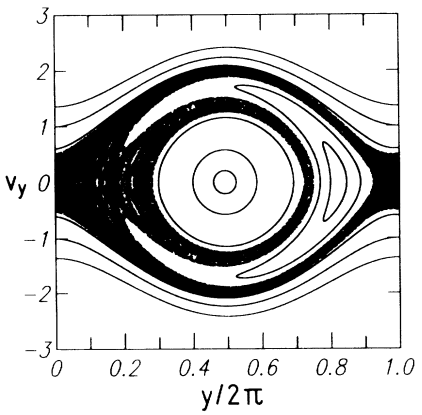

FIG. 4. Same as Fig. 2 for $\lambda=0.014$. Two-dimensional diffusion sets in as the KAM tori separating the two stochastic layers in Fig. 3 are destroyed. The connected stochastic region was generated by a single orbit.

and y diffusion is determined by the flux across two "golden" cantori. From work on the standard map[13] we may expect that it shows critical scaling behavior near λ_c with a power-law growth $(\lambda-\lambda_c)^{3.011722}$.

Finally we discuss the origin of the observed $1/f$ noise and anomalous diffusion. In these cases the Poincaré sections exhibit sufficiently large regular islands in the delocalized regions of the chaotic layers.[12] The islands are surrounded by daughter islands and a self-similar hierarchical arrangement where each island is encircled by barriers (low-flux cantori). This is also what one expects generically for a nonintegrable Hamiltonian system. A chaotic orbit may penetrate into this hierarchy of barriers and remain trapped for an arbitrarily long time thus causing long-time tails. More details of this mechanism will be given elsewhere.[12] For another model we have previously presented a statistical theory relating the algebraic free-path distribution to the island hierarchy.[10]

The parameter regimes considered here can be realized in lateral surface superlattices[5-8] (typical values $a=500$ nm, $\lambda_F=50$ nm). Our nonlinearity parameter λ [Eq. (5)] does not only depend on B and a, but also varies inversely with $V_0^{1/2}$. Using the technique of Winkler, Kotthaus, and Ploog[7] the amplitude of the superlattice potential can be varied between 0 and 1 eV by varying the gate voltage. It is therefore not a problem to reach values of λ between 10^{-3} and 10^{1} including the values considered here (e.g., $\lambda=2$ for $B=1$ T and $V_0=1$ meV). The chaotic fluctuation phenomena can dominate the current autocorrelation function and power spectrum at low temperatures only. For intrinsic reasons $1/f$ noise precludes a determination of its noise level. Thus a quantitative comparison of our $1/f$ mechanism with others is not possible.

We acknowledge useful discussions with J. E. Howard, J. P. Kotthaus, and M. Sherwin, financial support by Deutsche Forschungsgemeinschaft, and technical support by Rechenzentrum der Universität Regensburg.

[a]Present address.

[1]D. R. Hofstadter, Phys. Rev. B **14**, 2239 (1976).

[2]B. Simon, Adv. Appl. Math. **3**, 463 (1982).

[3]S. Ostlund and R. Pandit, Phys. Rev. B **29**, 1394 (1984).

[4]See, e.g., M. V. Berry, in *Topics in Nonlinear Dynamics,* edited by S. Jorna, AIP Conference Proceedings No. 46 (American Institute of Physics, New York, 1978), p. 16.

[5]H. Sakaki, K. Wagatsuma, J. Hamasaki, and S. Saito, Thin Solid Films **36**, 497 (1976); R. T. Bate, Bull. Am. Phys. Soc. **22**, 407 (1977); A. C. Warren, D. A. Antoniadis, H. I. Smith, and J. Melngailis, IEEE Electron. Device Lett. **6**, 294 (1985).

[6]R. R. Gerhardts, D. Weiss, and K. v. Klitzing, Phys. Rev. Lett. **62**, 1173 (1989).

[7]R. W. Winkler, J. P. Kotthaus, and K. Ploog, Phys. Rev. Lett. **62**, 1177 (1989).

[8]D. K. Ferry, G. Bernstein, and Wen-Ping Liu, in *Physics and Technology of Submicron Structures,* edited by H. Heinrich, G. Bauer, and F. Kuchar (Springer-Verlag, Berlin, 1988), p. 37; K. Ismail, W. Chu, A. Yen, D. A. Antoniadis, and H. I. Smith, Appl. Phys. Lett. **54**, 460 (1989); P. H. Beton, E. S. Alves, M. Henini, L. Eaves, P. C. Main, O. H. Hughes, G. A. Toombs, S. P. Beaumont, and C. D. W. Wilkinson (to be published); A. Lorke, J. P. Kotthaus, and K. Ploog (to be published).

[9]C. W. J. Beenakker, Phys. Rev. Lett. **62**, 2020 (1989); C. W. J. Beenakker and H. van Houten, Phys. Rev. Lett. **63**, 1857 (1989).

[10]T. Geisel, A. Zacherl, and G. Radons, Phys. Rev. Lett. **59**, 2503 (1987); Z. Phys. B **71**, 117 (1988).

[11]A. Zacherl, T. Geisel, J. Nierwetberg, and G. Radons, Phys. Lett. **114A**, 317 (1986).

[12]J. Wagenhuber, T. Geisel, P. Niebauer, and G. Obermair (to be published).

[13]R. S. MacKay, J. D. Meiss, and I. C. Percival, Physica (Amsterdam) **13D**, 55 (1984).

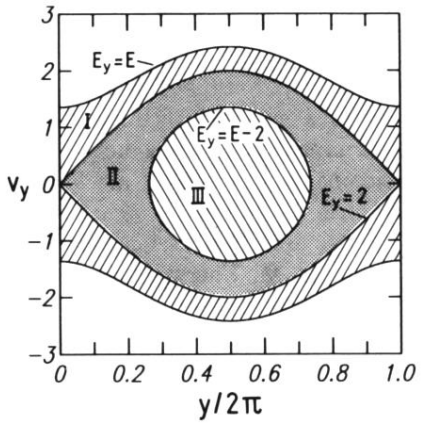

FIG. 2. Poincaré surface of section at the potential minimum for the zero-field case ($\lambda = 0$). Two separatrices divide the phase space into regions of delocalized (drifting) motions (I, III) and localized motions (II).